Statistical Methods in Surveying by Trilateration

William Navidi†,
William S. Murphy Jr.‡, and Willy Hereman†

†Department of Mathematical and Computer Sciences
Colorado School of Mines
Golden, Colorado 80401–1887

‡ U.S. Army TRADOC Analysis Center – Monterey
Naval Postgraduate School
P.O. Box 8692
Monterey, California 93943–0692

December 20, 1999

Keywords:

Iteratively reweighted least-squares, Quasi-likelihood, Monte-Carlo simulation, Trilateration, Computerized surveying, Global Positioning System (GPS)

Abstract

Trilateration techniques use distance measurements to survey the spatial coordinates of unknown positions. In practice, distances are measured with error, and statistical methods can quantify the uncertainty in the estimate of the unknown location. Three methods for estimating the three-dimensional position of a point via trilateration are presented: a linear least squares estimator, an iteratively reweighted least squares estimator, and a nonlinear least squares technique. In general, the nonlinear least squares technique performs best, but in some situations a linear estimator could in theory be constructed that would outperform it.

By eliminating the need to measure angles, trilateration facilitates the implementation of fully automated real-time positioning systems similar to the global positioning system (GPS). The methods presented in this paper are tested in the context of a realistic positioning problem that was posed by the Thunder Basin Coal Company in Wright, Wyoming.

1 Introduction

Thunder Basin Coal Company (TBCC), based in Wright, Wyoming, wished to develop a fully automated surveying system to accurately determine the three-dimensional position of equipment in an open pit mine. Standard surveying techniques are based on measurement of angles and a baseline distance to determine the unknown position components (the latitude x, the longitude y, and the altitude z) of a point relative to a fixed coordinate system. Such *triangulation* methods are laborious, expensive and slow. The advent of accurate electronic distance measuring equipment and high speed computers enables surveyors to replace angular measurements with distance measurements by using the *trilateration* surveying technique (Laurila 1983; Moffitt and Bouchard, 1992; Savidge 1980).

Several advanced and widely used positioning systems were considered for TBCC's problem, in particular, the Global Positioning System (GPS) (Leick, 1990; Parkinson and Spilker, 1996). However, TBCC determined that with GPS as it is available to the civil community, the vertical position accuracy is insufficient. Accurate elevations are key in mining applications. For example, in dynamic blasting, where the soil atop of the coal is removed via controlled explosions, both accurate positioning of the drill and precise measurement of the depth of the bore-hole are essential.

As an alternative to GPS, the engineers at TBCC proposed placing a system of radio beacons at known locations on the rim of the mine. The coordinates of the beacons would be carefully determined with conventional surveying methods to nearly perfect accuracy. To determine the position of a piece of equipment in the mine, each beacon would transmit a radio signal to the target point, then receive its reflection. The distance between a beacon and the target point can be computed as a function of the measured time between transmission and reception. The spatial coordinates of the target point would then computed from the measured distances to the various beacons. An experimental setup was put into place at TBCC in 1993. A diagram of this setup is presented in Figure 1.

Electronic systems and electro-optical instruments for distance measurements are fairly accurate, but measurement error needs to be taken into account. TBCC estimated that the magnitude of a typical error on the distance from the beacon to the target point would be about 0.5 feet. Because of this, there will generally be no point in space whose actual distances to the known beacons correspond to the measured ones, so methods based on exact distances will fail to yield a solution.

Various deterministic procedures have been proposed for approximating the coordinates of the target point (Danial and Krauthammer, 1980; Laurila 1983; Mezera, 1983; Moffitt and Bouchard, 1992). A statistical approach that takes measurement error into account can produce estimates for the coordinates of the target point along with a confidence region for its position.

In principle, many repeated measurements could be made from each beacon. It is possible that such a sequence would exhibit some degree of autocorrelation. The methods described here assume that all measurements are independent. This could certainly be achieved by taking only one measurement per beacon, and we adopt this conservative approach in our simulation studies. If sequences of nearly independent measurements can be obtained from each beacon, the accuracy of the methods we describe would be considerably enhanced.

The usefulness of statistical methods for the three-dimensional trilateration positioning problem is not restricted to mining applications that use radio signals to measure distances. Our algorithms can be utilized in any system that involves distance measurements obtained with radar, lasers, or manual measurement. Indeed, there are numerous real-world applications where triangulation methods for determining positions in a timely, accurate, and cost effective manner are out of the question. Trilateration methods are the most appropriate in a variety of circumstances that involve aircraft, land vehicle, marine vessel, and spacecraft navigation (Leick, 1990; Parkinson and Spilker, 1996). New and innovative applications of high-precision trilateration include dredging operations, precision farming, underwater positioning, precision landing of aircraft, vehicle tracking systems, construction related surveying inside large building shells, monitoring of distortion of large objects such as dams and bridges, robotics applications, guidance systems for smart weapons.

In this paper we present three statistical approaches to the trilateration problem, together with detailed comparisons of their performance. The paper is organized as follows. In section 2 we present two linear least squares procedures. The first involves an exact linearization of the problem, and estimation by ordinary least squares (OLS). The second method uses iteratively reweighted least squares (IRLS) in an effort to improve on the OLS estimator. In section 3, we turn to the full non-linear problem and treat it with a non-linear least squares (NLLS) technique. In section 4 we compare the accuracy of the procedures with a Monte-Carlo simulation using actual beacon locations from TBCC. In section 5 we describe existing software for NLLS estimators as well as our own implementation. In section 6 we discuss our results and present conclusions.

The statistical methods we present are for the most part familiar least-squares procedures. To obtain a linear least-squares model for trilateration, we developed a new method of exact linearization. Non-linear least squares models have been discussed by Wolf and Ghilani (1997). We show how these results can be extended to unequal variance situations, using the theory of quasi-likelihood estimation.

2 Linear Least-Squares

2.1 Constructing a Linear Model

With reference to Figure 1, let n denote the total number of measurements taken at all beacons combined. Let $\theta = (x, y, z)$ denote the spatial coordinates of the target point. Let $B_i = (x_i, y_i, z_i)$ be the exact location of the beacon at which the ith measurement is taken. Define

$$d_i(\theta) = \sqrt{(x_i - x)^2 + (y_i - y)^2 + (z_i - z)^2},$$

the true distance from the ith beacon to the target point. In order to ensure identifiability, we assume that there are enough beacons so that if $\theta \neq \theta'$, then there is at least one i for which $d_i(\theta) \neq d_i(\theta')$. Let r_i be the measured distance from the ith beacon to the target point. We assume that $r_i = d_i(\theta) + \varepsilon_i$, where the ε_i are independent, with $\mathrm{E}(\varepsilon_i) = 0$ and $\mathrm{Var}(\varepsilon_i) = \sigma^2$. We discuss alternative assumptions on the variance in section 6.2. Notice that we do not make any distributional assumptions, such as normality, on ε_i.

The regression equations

$$d_i(\theta) = \mathrm{E}(r_i|x, y, z) = \sqrt{(x - x_i)^2 + (y - y_i)^2 + (z - z_i)^2}$$

are non-linear in the unknowns x, y, z, but a linear regression equation can be developed as shown below. Alternate methods of linearization have been proposed by Laurila (1983), and Parkinson and Spilker (1996).

Let (x_r, y_r, z_r) be the coordinates of any point in $\mathbf{R}^3$, which we will refer to as the reference point. Now for each of the n points (x_i, y_i, z_i), write

$$d_i(\theta)^2 = (x - x_r + x_r - x_i)^2 + (y - y_r + y_r - y_i)^2 + (z - z_r + z_r - z_i)^2. \tag{1}$$

Let

$$d_{ir} = \sqrt{(x_i - x_r)^2 + (y_i - y_r)^2 + (z_i - z_r)^2},$$

the distance between the reference point and the location of the beacon at which the ith measurement was taken. Let

$$d_r(\theta) = \sqrt{(x - x_r)^2 + (y - y_r)^2 + (z - z_r)^2},$$

the distance between the reference point and the target point (x, y, z). Expanding and regrouping terms in (1), we obtain

$$2[(x - x_r)(x_i - x_r) + (y - y_r)(y_i - y_r) + (z - z_r)(z_i - z_r)] = d_r(\theta)^2 + {d_{ir}}^2 - d_i(\theta)^2. \tag{2}$$

Define the matrix

$$\mathbf{X} = \begin{bmatrix} 1 & 2(x_1 - x_r) & 2(y_1 - y_r) & 2(z_1 - z_r) \\ 1 & 2(x_2 - x_r) & 2(y_2 - y_r) & 2(z_2 - z_r) \\ \vdots & \vdots & \vdots & \vdots \\ 1 & 2(x_n - x_r) & 2(y_n - y_r) & 2(z_n - z_r) \end{bmatrix}. \tag{3}$$

Define the parameter vector

$$\beta = \begin{bmatrix} -d_r(\theta)^2 - \sigma^2 \\ x - x_r \\ y - y_r \\ z - z_r \end{bmatrix}. \tag{4}$$

Define

$$Y_i = {d_{ir}}^2 - {r_i}^2, \tag{5}$$

and let $\mathbf{Y}$ denote the vector whose ith component is Y_i. Since the ${d_{ir}}^2$ are known constants, and since $\mathrm{E}({r_i}^2|x, y, z) = d_i(\theta)^2 + \sigma^2$, it follows that $\mathrm{E}(Y_i) = {d_{ir}}^2 - d_i(\theta)^2 - \sigma^2$, so that

$$\mathrm{E}(\mathbf{Y}) = \mathbf{X}\beta. \tag{6}$$

The Y_i are independent, and

$$\mathrm{Var}(Y_i) = \mathrm{Var}({r_i}^2) = \mathrm{Var}([d_i(\theta)+\varepsilon_i]^2) = \mathrm{Var}(2d_i(\theta)\varepsilon_i + {\varepsilon_i}^2) = 4d_i(\theta)^2\sigma^2 + 4d_i(\theta)\mu_3 + \mu_4 - \sigma^4, \tag{7}$$

where σ^2, μ_3, and μ_4 are the second, third, and fourth moments of the distribution of the ε_i.

The first component of β contains a non-linear function of the components of $\theta = (x, y, z)$, so it appears that this is not a linear regression. For now, we ignore the functional dependence, and treat the first component as a free parameter. It will be shown in Section 2.2 that this does not affect the estimation of θ.

We describe below a linear regression model that produces the OLS estimator of θ. Since the variances of the Y_i are not identical, this estimator is not necessarily optimal. In principle, one can attempt to improve on the performance of the OLS estimator with an IRLS regression, in which the variances of the Y_i are estimated along with θ in an iterative fashion. We discuss this possibility in Section 2.3.

2.2 The Ordinary Least Squares Estimator

To make the regression equation (6) linear in the unknowns x, y, z, note that the span of the columns of $\mathbf{X}$ does not depend on the choice of the reference point. Therefore the value of $\mathbf{X}\hat{\beta}$ does not depend on the reference point, and it follows easily that the values of the estimates $\hat{x}$, $\hat{y}$, and $\hat{z}$ do not depend on the choice of the reference point. This suggests using the value $\bar{\theta} = (\bar{x}, \bar{y}, \bar{z})$ as the reference point. This choice makes the rightmost three columns of $\mathbf{X}$ orthogonal to the column of ones, allowing it and the first component of (4) to be dropped from the model without affecting the estimation of $\theta = (x, y, z)$.

Define $\mathbf{X}_*$ to be the matrix consisting of the rightmost three columns of (3), and $\mathbf{Y}_* = \mathbf{Y} + \mathbf{X}_*\bar{\theta}$. Then

$$\mathrm{E}(\mathbf{Y}_*) = \mathbf{X}_*\theta, \tag{8}$$

and the OLS estimator of θ is

$$\hat{\theta} = (\mathbf{X}_*^T\mathbf{X}_*)^{-1}\mathbf{X}_*^T\mathbf{Y}_*. \tag{9}$$

Equation (8) guarantees that $\hat{\theta}$ will be unbiased, with covariance matrix

$$\mathrm{Cov}(\hat{\theta}) = (\mathbf{X}_*^T\mathbf{X}_*)^{-1}\mathbf{X}_*^T\mathbf{\Sigma}\mathbf{X}_*(\mathbf{X}_*^T\mathbf{X}_*)^{-1}, \tag{10}$$

where $\mathbf{\Sigma}$ is the diagonal matrix whose ith diagonal element is $\mathrm{Var}(Y_i)$, given by (7). The elements of $\mathbf{X}_*$ depend only on the known locations of the beacons, and the elements of $\mathbf{\Sigma}$ depend on the distances from the target point to the beacons. Thus for fixed beacon positions, the variances of the estimates of the coordinates of the target point will increase as the distances from the target point to the beacons increase.

Since $\mathbf{\Sigma}$ is unknown, we cannot use (10) to compute $\mathrm{Cov}(\hat{\theta})$. Instead, we can compute the conventional OLS estimate of $\mathrm{Cov}(\hat{\theta})$ as follows. We first compute the residual mean square

s^2. Since the design matrix $\mathbf{X}_*$ has no intercept, it is necessary to regress it out separately in computing s^2. Thus s^2 is given by

$$s^2 = \frac{1}{n-4}\sum_{i=1}^{n}(Y_i - \bar{Y} - \hat{Y}_i)^2. \tag{11}$$

Here $\hat{\mathbf{Y}} = \mathbf{X}_*\hat{\theta}$.

Now we can compute the conventional OLS estimate of $\mathrm{Cov}(\hat{\theta})$, which is $s^2(\mathbf{X}_*^T\mathbf{X}_*)^{-1}$. The trace of this matrix estimates the mean squared error (MSE) of $\hat{\theta}$, which is the expected squared distance from the target point to its estimate. Thus

$$\mathrm{MSE}(\hat{\theta}) = \mathrm{Trace}[s^2(\mathbf{X}_*^T\mathbf{X}_*)^{-1}]. \tag{12}$$

We can also compute the conventional 95% confidence ellipsoid for the true value $\theta = (x, y, z)$. This is the set

$$S = \{\theta \mid (\hat{\theta} - \theta)^T(s^{-2}\mathbf{X}_*^T\mathbf{X}_*)(\hat{\theta} - \theta) \ < 3F_{3,\ n-4,\ .95}\}, \tag{13}$$

where $F_{3,\ n-4,\ .95}$ is the 95th percentile of the $\mathrm{F}_{3,\ n-4}$ distribution.

2.3 Iteratively Reweighted Least Squares

Since the variances of the Y_i are unequal, the OLS estimator may be improved upon. The variances of the Y_i compose the elements of the diagonal matrix $\mathbf{\Sigma}$. If these variances were known, then the best linear estimator of β would be given by

$$\hat{\beta}_{opt} = (\mathbf{X}^T\mathbf{\Sigma}^{-1}\mathbf{X})^{-1}\mathbf{X}^{\mathbf{T}}\mathbf{\Sigma}^{-1}\mathbf{Y}, \tag{14}$$

with covariance matrix

$$\mathrm{Cov}(\hat{\beta}_{opt}) = (\mathbf{X}^T\mathbf{\Sigma}^{-1}\mathbf{X})^{-1}. \tag{15}$$

The best linear estimate $\hat{\theta}_{opt}$ of θ consists of the last three components of $\hat{\beta}_{opt}$. Since the elements of $\mathbf{\Sigma}$ are unknown, we cannot compute $\hat{\beta}_{opt}$. However, we can attempt to approximate it by IRLS. To perform this method, we initialize an estimate $\hat{\mathbf{\Sigma}}$ to the identity matrix $\mathbf{I}$, and compute $\hat{\beta}$ by (14). We then use the elements of $\hat{\beta}$ to update the estimate $\hat{\mathbf{\Sigma}}$, and recompute $\hat{\beta}$. This process is iterated to convergence.

In principle, it is possible to compute the IRLS estimate $\hat{\theta}$ from a truly linear model, as in the case of the OLS estimator. Let $\hat{\mathbf{\Sigma}}_n$ be the estimate of $\mathbf{\Sigma}$ after n iterations. For the $n+1st$ iteration, define the reference point θ_r by

$$\theta_r = \frac{\sum_{i=1}^{n} B_i/\hat{\sigma}_i}{\sum_{i=1}^{n} 1/\hat{\sigma}_i},$$

where $B_i = (x_i,\ y_i,\ z_i)$ are the coordinates of the beacon from which the ith measurement was taken, and $\hat{\sigma}_i$ is the square root of the ith diagonal element of $\hat{\mathbf{\Sigma}}_n$. Then the first column of the matrix $\hat{\mathbf{\Sigma}}^{-1/2}\mathbf{X}$ is orthogonal to the other three, so it can be dropped from the model, along with the first component of (4). In practice, this recomputation of the reference point and the matrix $\mathbf{X}$ at each iteration is unnecessary. Identical results will be obtained by using the full design matrix (3), and estimating $\hat{\beta}$ at each iteration. Upon convergence the last three components of $\hat{\beta}$ form the IRLS estimator of θ.

To update the estimate $\hat{\mathbf{\Sigma}}$, we express the ith diagonal element of $\mathbf{\Sigma}$ in terms of the moments of the ε_i:

$$\Sigma_{ii} = 4d_i(\theta)^2\sigma^2 + 4d_i(\theta)\mu_3 + \mu_4 - \sigma^4. \tag{16}$$

Let the components of $\hat{\theta}$ be denoted by $(\hat{x}, \hat{y}, \hat{z})$. These components are used to estimate each of the quantities on the right side of (16). Specifically, $d_i(\theta)$ is estimated with $d_i(\hat{\theta})$, the distance from the beacon at which the ith measurement was made to the point $\hat{\theta}$. The moments σ^2, μ_3, μ_4 can be expressed in terms of the $d_i(\theta)$ and the moments of the r_i. For each measurement i, we have

$$\sigma^2 = \mathrm{E}({r_i}^2) - d_i(\theta)^2, \tag{17}$$

$$\mu_3 = \mathrm{E}({r_i}^3) - d_i(\theta)^3 - 3\sigma^2 d_i(\theta), \tag{18}$$

$$\mu_4 = \mathrm{E}({r_i}^4) - d_i(\theta)^4 - 6\sigma^2 d_i(\theta)^2 - 4\mu_3 d_i(\theta). \tag{19}$$

The estimates are given by

$$\hat{\sigma}^2 = \frac{1}{n}\sum_{i=1}^{n} {r_i}^2 - d_i(\hat{\theta})^2, \tag{20}$$

$$\hat{\mu}_3 = \frac{1}{n}\sum_{i=1}^{n} {r_i}^3 - d_i(\hat{\theta})^3 - 3\hat{\sigma}^2 d_i(\hat{\theta}), \tag{21}$$

$$\hat{\mu}_4 = \frac{1}{n}\sum_{i=1}^{n} {r_i}^4 - d_i(\hat{\theta})^4 - 6\hat{\sigma}^2 d_i(\hat{\theta})^2 - 4\hat{\mu}^3 d_i(\hat{\theta}). \tag{22}$$

When the sample size is small, it turns out that if all the moment estimators are used in (16), the IRLS procedure is quite unstable, and frequently fails to converge. An approximate method, that is considerably more stable, is obtained by ignoring moments higher than the second. Thus we approximate

$$\Sigma_{ii} = 4 d_i(\theta)^2 \sigma^2. \tag{23}$$

and estimate σ^2 by (20). The justification for this approximation is that the moments of the measurement error should be much less than the true distance. Thus the right hand side of (16) is dominated by its first term.

After convergence, the covariance matrix of $\hat{\theta}$ is estimated with $(\mathbf{X}_*^T \hat{\mathbf{\Sigma}}^{-1} \mathbf{X}_*)^{-1}$. By analogy with (12) and (13), we estimate the MSE of $\hat{\theta}$ with

$$\mathrm{MSE}(\hat{\theta}) = \mathrm{Trace}[\mathbf{X}_*^T \hat{\mathbf{\Sigma}}^{-1} \mathbf{X}_*]^{-1}, \tag{24}$$

and the nominal 95% confidence region is given by

$$S = \{\theta \mid (\hat{\theta} - \theta)^T \mathbf{X}_*^T \hat{\mathbf{\Sigma}}^{-1} \mathbf{X}_* (\hat{\theta} - \theta) \ < 3F_{3,\ n-4,\ .95}\}. \tag{25}$$

3 Non-linear Least-Squares

The OLS estimate minimizes the quantity $\sum_{i=1}^{n}[{d_{ir}}^2 - {r_i}^2 - d_i(\theta)^2]^2$. A simpler sum of squares is given by

$$F(\theta) = \sum_{i=1}^{n}[r_i - d_i(\theta)]^2 = \sum_{i=1}^{n}\left(r_i - \sqrt{(x_i - x)^2 + (y_i - y)^2 + (z_i - z)^2}\right)^2. \quad (26)$$

The NLLS estimator $\hat{\theta}$ of θ is the minimizer of F. The function $F(\theta)$ is a quasi-likelihood function (McCullagh and Nelder, 1989).

If we define $\mathbf{J}(\theta)$ to be the $n \times 3$ matrix

$$\mathbf{J}(\theta) = \begin{pmatrix} \frac{\partial d_1(\theta)}{\partial x} & \frac{\partial d_1(\theta)}{\partial y} & \frac{\partial d_1(\theta)}{\partial z} \\ \frac{\partial d_2(\theta)}{\partial x} & \frac{\partial d_2(\theta)}{\partial y} & \frac{\partial d_2(\theta)}{\partial z} \\ \vdots & \vdots & \vdots \\ \frac{\partial d_n(\theta)}{\partial x} & \frac{\partial d_n(\theta)}{\partial y} & \frac{\partial d_n(\theta)}{\partial z} \end{pmatrix}, \quad (27)$$

it then follows from McCullagh and Nelder (1989, pp. 327–328), that $\hat{\theta}$ is asymptotically normal and unbiased, with asymptotic covariance matrix $\sigma^2[\mathbf{J}(\theta)^T\mathbf{J}(\theta)]^{-1}$.

In practice, σ^2 is estimated with

$$\frac{1}{n-3}\sum_{i=1}^{n}[r_i - d_i(\hat{\theta})]^2,$$

and the asymptotic covariance matrix is estimated with

$$\text{Cov}(\hat{\theta}) = \hat{\sigma}^2[\mathbf{J}(\hat{\theta})^T\mathbf{J}(\hat{\theta})]^{-1}. \quad (28)$$

Denoting the components of θ by $(x,\ y,\ z)$, the matrix $\mathbf{J}(\theta)^T\mathbf{J}(\theta)$ can be written as

$$\mathbf{J}(\theta)^T\mathbf{J}(\theta) = \begin{pmatrix} \sum_{i=1}^n \frac{(x-x_i)^2}{d_i(\theta)^2} & \sum_{i=1}^n \frac{(x-x_i)(y-y_i)}{d_i(\theta)^2} & \sum_{i=1}^n \frac{(x-x_i)(z-z_i)}{d_i(\theta)^2} \\ \sum_{i=1}^n \frac{(x-x_i)(y-y_i)}{d_i(\theta)^2} & \sum_{i=1}^n \frac{(y-y_i)^2}{d_i(\theta)^2} & \sum_{i=1}^n \frac{(y-y_i)(z-z_i)}{d_i(\theta)^2} \\ \sum_{i=1}^n \frac{(x-x_i)(z-z_i)}{d_i(\theta)^2} & \sum_{i=1}^n \frac{(y-y_i)(z-z_i)}{d_i(\theta)^2} & \sum_{i=1}^n \frac{(z-z_i)^2}{d_i(\theta)^2} \end{pmatrix}. \quad (29)$$

The diagonal elements of $\mathbf{J}(\theta)^T\mathbf{J}(\theta)$ can be described as follows. For each beacon, the squared distance between the target point and the beacon is divided into the squared distance between the x-coordinates (or the y- or z-coordinates). Then the quantities are summed across beacons. Since the asymptotic covariance of $\hat{\theta}$ is proportional to the inverse of $\mathbf{J}(\theta)^T\mathbf{J}(\theta)$, it follows that the NLLS estimator will have smaller MSE when the x, y, and z components of the distances from the target point to the beacons are approximately equal, and larger MSE for target points one of whose coordinates is substantially closer to the beacons than the other coordinates are.

This phenomenon can be seen most clearly in the situation where the beacons are placed orthogonally to one another, so that the off diagonal elements of $\mathbf{J}(\theta)^T\mathbf{J}(\theta)$ are equal to 0. Then the asymptotic variances of the estimates of the x, y, and z coordinates of the target point are given by $\left[\sum_{i=1}^n \frac{(x-x_i)^2}{d_i(\theta)^2}\right]^{-1}$, $\left[\sum_{i=1}^n \frac{(y-y_i)^2}{d_i(\theta)^2}\right]^{-1}$, and $\left[\sum_{i=1}^n \frac{(z-z_i)^2}{d_i(\theta)^2}\right]^{-1}$, respectively, where $d_i(\theta)^2 = (x_i - x)^2 + (y_i - y)^2 + (z_i - z)^2$.

4 Simulation Results

Analytic calculations provide asymptotic estimates of variance, which are approximations to the true variances for finite samples. In order to assess the accuracy of the asymptotic variance estimates, and to compare the performance of the various methods, simulation studies are needed. We performed several simulation studies, based on information and data provided by TBCC. They suggested that eight fixed-position radio beacons would be feasible in terms of cost. The beacons $B_1, ..., B_8$ are installed on the rim of the mine, and their actual locations are determined primarily by topographic considerations. We used the locations suggested by TBCC, which are shown in Table 1. The coordinates given for each of the eight beacons are accurate distances in feet with respect to a fixed reference point in western Wyoming that was chosen by TBCC. Figure 2 presents a perspective view of the eight beacons.

To study the ways in which the performance of the estimates varies with the location of the target point, we considered 1000 target points, located in a rectangular grid. Figure 3 shows the grid of 1000 target points. For each of the 1000 target points, we constructed 10000 data sets. Each data set consisted of one measurement from each beacon. To simulate the conditions anticipated in TBCC's mine, the measurements were generated by adding to the true distance a random error from a uniform distribution on the interval $(-0.5, 0.5)$.

For each data set, we computed the OLS estimate (9), the nominal estimate of its MSE in (12), the IRLS estimate, the nominal estimate of its MSE in (24), the NLLS estimate, and the nominal estimate of its MSE in (28).

In Table 2 we present the results. To explain the entries in that table, let θ_j $(j = 1, ..., 1000)$ be the target points. Let $\hat{\theta}_j$ represent an estimator (OLS, IRLS, or NLLS) of θ_j, and let $\hat{\theta}_j(r)$ $(r = 1, ..., 10000)$, be the value of $\hat{\theta}_j$ computed from the rth data set. We take the "true" MSE of $\hat{\theta}_j$ to be the quantity

$$\text{MSE} = \frac{1}{10000} \sum_{r=1}^{10000} [\hat{\theta}_j(r) - \theta_j]^2. \tag{30}$$

For each data set r, we computed the nominal MSE of $\hat{\theta}_j$. We denote these quantities by $\text{NMSE}_j(r)$ $(r = 1, ..., 10000)$. The performance of the nominal MSE at any given point j can be assessed through the quantity $\overline{\mathrm{NMSE}}_j = \sum_{r=1}^{10000} \mathrm{NMSE}_j(r)/10000$.

The column labeled "RMSE" in Table 2 presents the quantity $\sqrt{\sum_{j=1}^{1000} \mathrm{MSE}_j}$ for each of the three estimators. The column labeled "Nominal RMSE" presents the quantity $\sqrt{\sum_{j=1}^{1000} \overline{\mathrm{NMSE}}_j}$ for each of the three estimators. The column labeled "Coverage Probability" presents the proportion of nominal 95% confidence regions, taken over all data sets and target points, that covered the true value.

Table 2 shows clearly that in this example, the NLLS estimator is best in terms of RMSE, followed by the IRLS and OLS estimators. In fact, the NLLS estimator had smaller mean squared error for each of the 1000 target points than did either of the linear estimators. TBCC hoped to develop a method that would enable the three coordinates of positions to be estimated within a tolerance of five feet. Table 2 shows that the NLLS method achieved this goal in terms of MSE. Comparing the first and second columns of Table 2 shows that the nominal mean squared error is on the average quite close to the true value for the OLS and NLLS estimators, but is biased severely upward for the IRLS estimator. The true coverage probabilities were close to the nominal 95% level for all three estimators. Since the nominal MSE is biased slightly downward for the OLS and NLLS estimators , the coverage probabilities are slightly low. For the IRLS estimator, the nominal MSE is biased severely upward, yet the average coverage probability is only slightly high. This is due partly to the fact that the coverage probability is bounded above by 1, so no point can have true coverage much greater than the nominal 95% level, and partly to the fact that there were a few target points for which the true coverage probability was quite low.

Table 2 summarizes the performances of the estimators over all 1000 target points. To describe how the behavior of the estimators varied over the points, we present some plots. Figure 4 presents a scatterplot of quantities $\sqrt{\mathrm{MSE}_j}$ for the IRLS estimator vs. the corresponding quantities for the OLS estimator. The IRLS estimator outperforms the OLS estimator at each of the 1000 target points. Figure 5 presents the equivalent comparison of the NLLS estimator with the IRLS estimator. The NLLS estimator outperforms the IRLS estimator at each of the 1000 target points.

Figures 6, 7, and 8 present histograms of the true coverage probability for the nominal 95% confidence regions for the OLS, IRLS, and NLLS procedures, respectively. The area under a given region of a histogram indicates the proportion of the 1000 target points whose true coverage probabilities fell in that region. The true coverage probabilities for the OLS and NLLS estimators are concentrated slightly below the nominal 95% value. For the IRLS estimator, most of the target points had coverage probabilities well above 95%, while a few had values well below.

The NLLS method provided the most accurate results of all methods developed and examined. The NLLS method performed least well at target points near the top of the mine, where the distances between target points and beacons were very small in the z-direction compared to the distances in the x- and y-directions. Still, the NLLS method outperformed the linear methods even at the top of the mine.

5 Numerical Methods and Implementation

Minimizing the sum of the square errors is a common problem in applied mathematics for which various algorithms (McKeown 1975) as well as software packages are available. Numerous approaches can be taken, from simple to very complicated (Mikhail 1976). For the linear problems, we used Gauss-Jordan elimination (Press, et al., 1992) to solve the normal equations. This approach is generally inefficient, but was feasible because the dimensions of the problems were small. For the non-linear least squares minimization, we used NAG subroutine E04KAF (NAG, 1991), a quasi-Newton algorithm that requires calculation of the first derivatives of the objective function. Another iterative procedure for computing the NLLS estimate was discussed in Laurila (1983, pp. 187-88).

We also implemented our own algorithms for this problem in Borland C++. We only considered the case for which $F_{\min} > 0$, corresponding to $n > 3$. We used Newton iteration to find the NLLS estimator $\hat{\theta} = (\hat{x}, \hat{y}, \hat{z})$ which minimizes

$$F(\theta) = F(x,y,z) = \sum_{i=1}^{n} f_i(x,y,z)^2, \tag{31}$$

where

$$f_i(x,y,z) = f_i(\theta) = d_i(\theta) - r_i = \sqrt{(x_i - x)^2 + (y_i - y)^2 + (z_i - z)^2} - r_i. \tag{32}$$

The function $F(\theta)$ was defined in (26), and n is the number of beacons.

Differentiating (31) with respect to x yields

$$\frac{\partial F(\theta)}{\partial x} = 2\sum_{i=1}^{n} f_i \frac{\partial f_i(\theta)}{\partial x} = 2\sum_{i=1}^{n} f_i \frac{\partial d_i(\theta)}{\partial x}. \tag{33}$$

The formulae for the partials with respect to y and z are similar. Recall that $\mathbf{J}(\theta)$ is the $n \times 3$ matrix given by (27). Furthermore,

$$\mathbf{f}(\theta) = \begin{pmatrix} f_1(\theta) \\ f_2(\theta) \\ \vdots \\ f_n(\theta) \end{pmatrix}, \quad \nabla F(\theta) = \begin{pmatrix} \frac{\partial F(\theta)}{\partial x} \\ \frac{\partial F(\theta)}{\partial y} \\ \frac{\partial F(\theta)}{\partial z} \end{pmatrix}, \quad \mathbf{J}(\theta)^T \mathbf{f}(\theta) = \begin{pmatrix} \sum_{i=1}^{n} \frac{(x - x_i) f_i(\theta)}{d_i(\theta)} \\ \sum_{i=1}^{n} \frac{(y - y_i) f_i(\theta)}{d_i(\theta)} \\ \sum_{i=1}^{n} \frac{(z - z_i) f_i(\theta)}{d_i(\theta)} \end{pmatrix}. \tag{34}$$

We must solve

$$\nabla F(\theta) = 2\mathbf{J}(\theta)^T \mathbf{f}(\theta) = \mathbf{0}. \tag{35}$$

Newton's method applied to (35) leads to the iteration procedure:

$$\theta_{\{k+1\}} = \theta_{\{k\}} - [\mathbf{J}(\theta_{\{k\}})^T \mathbf{J}(\theta_{\{k\}})]^{-1} \mathbf{J}(\theta_{\{k\}})^T \mathbf{f}(\theta_{\{k\}}), \tag{36}$$

where $\theta_{\{k\}}$ denotes the kth estimate to the position vector $\theta = [x, y, z]^T$. The explicit expression for $\mathbf{J}(\theta)^T \mathbf{J}(\theta)$ was given in (29). A reasonably accurate initial guess, $\theta_{\{1\}}$, for $\hat{\theta}$ is the OLS estimate given in (9). Starting with $\theta_{\{1\}}$, the least squares (36) is iterated until the change in the estimate, $\theta_{\{k+1\}} - \theta_{\{k\}}$, is sufficiently small.

In practice this type of iteration works fast, in particular when the matrix $\mathbf{J}(\theta_{\{k\}})^T \mathbf{J}(\theta_{\{k\}})$ is augmented by a diagonal matrix which effectively biases the search direction towards that of *steepest decent*. Levenberg and Marquardt (Lawson and Hanson, 1974) developed this improvement.

6 Discussion

6.1 Comparison of Linear and Non-linear Estimators

To gain insight into the superior performance of the NLLS estimator, recall that θ denotes the target point, and that B_i denotes the location of the beacon at which the ith measurement was taken. Let $\bar{B} = \frac{1}{n} \sum_{i=1}^{n} B_i$.

The asymptotic covariance matrix of the NLLS estimate is $\sigma^2 [\mathbf{J}(\theta)^T \mathbf{J}(\theta)]^{-1}$. We compare this with the theoretically best covariance matrix $(\mathbf{X}_*^T \mathbf{\Sigma}^{-1} \mathbf{X}_*)^{-1}$ for a linear estimator. Recall that $\mathbf{\Sigma}$ is the diagonal matrix with elements given by (7), and $\mathbf{X}_*$ is the design matrix given by the rightmost three columns of (3).

We can write

$$\sigma^2 [\mathbf{J}(\theta)^T \mathbf{J}(\theta)]^{-1} = \sigma^2 \left[\sum_{i=1}^{n} \frac{(B_i - \theta)(B_i - \theta)^T}{d_i(\theta)^2} \right]^{-1}, \tag{37}$$

and using the approximation $\Sigma_{ii} = 4d_i(\theta)^2\sigma^2$,

$$(\mathbf{X}_*^T\mathbf{\Sigma}^{-1}\mathbf{X}_*)^{-1} = \sigma^2\left[\sum_{i=1}^{n}\frac{(B_i-\bar{B})(B_i-\bar{B})^T}{d_i(\theta)^2}\right]^{-1}. \tag{38}$$

Consider the difference between the inverses of these matrices:

$$\mathbf{J}(\theta)^T\mathbf{J}(\theta)/\sigma^2 - \mathbf{X}_*^T\mathbf{\Sigma}^{-1}\mathbf{X}_* = \frac{1}{\sigma^2}\sum_{i=1}^{n}\left[\frac{(B_i-\theta)(B_i-\theta)^T-(B_i-\bar{B})(B_i-\bar{B})^T}{d_i(\theta)^2}\right]. \tag{39}$$

The quantity in the brackets is easily shown to be positive definite. Therefore, if the $d_i(\theta)$ were identical, the asymptotic variance of any linear combination of the components of the NLLS estimator would be smaller than the variance of the corresponding linear estimator. Since the $d_i(\theta)$ are not identical, the NLLS estimator can be improved upon, in theory, at some target points. Of the 1000 target points used in our simulation, there were four points for which the trace of the matrix $(\mathbf{X}_*^T\mathbf{\Sigma}^{-1}\mathbf{X}_*)^{-1}$ was less than the trace of $\sigma^2[\mathbf{J}(\theta)^T\mathbf{J}(\theta)]^{-1}$. These points were all at the top of the grid, where the target z value was close to the z-coordinates z_i for the beacons. At these points, a linear estimator could in theory be constructed that would outperform the non-linear estimator. Our simulation study showed that in fact the non-linear procedure outperformed both the OLS and the IRLS estimators at every one of the target points. This shows that neither of the linear estimators had a covariance matrix sufficiently close to the optimal linear covariance matrix.

6.2 Alternative Models for Measurement Error

In some situations, it might be reasonable to assume that the magnitude of measurement errors tend to be proportional to the true distance being measured. In this case we would assume that Var $(\varepsilon_i) = \sigma^2 d_i(\theta)^2$.

It is not clear whether a reasonable linear estimator can be constructed in this case. The expectation of the quantity Y_i defined in (5) depends on the products of the coordinates of the target point θ with σ^2, so it cannot be used as the dependent variable in a linear model unless the value of σ^2 is known.

It is easy, however, to construct non-linear estimators. The most obvious approach might be to minimize the sum of squares

$$G(\theta) = \sum_{i=1}^{n} \left[\frac{r_i - d_i(\theta)}{d_i(\theta)} \right]^2 . \tag{40}$$

The estimator obtained by this approach is asymptotically normal, and it is possible to derive the asymptotic covariance matrix in the usual way, by computing the one-term Taylor series expansion of the gradient of $G(\theta)$. The asymptotic covariance of this estimator is somewhat intractable, however, and involves third and fourth order moments of the ε_i, for which accurate estimation may not be possible.

The better approach in this situation is the quasi-likelihood approach. The appropriate quasi-likelihood estimator is found by minimizing

$$\sum_{i=1}^{n} \frac{r_i}{d_i(\theta)} - \log[d_i(\theta)]. \tag{41}$$

See McCullagh and Nelder (1989) for a derivation. Let $\mathbf{V}$ denote the diagonal matrix whose ith diagonal element is equal to $d_i(\theta)^2$, so that $\sigma^2\mathbf{V}$ is the covariance matrix of the r_i. Then the asymptotic covariance of the quasi maximum likelihood estimator (McCullagh and Nelder, 1989) is given by $\sigma^2[\mathbf{J}(\theta)^T\mathbf{V}^{-1}\mathbf{J}(\theta)]^{-1}$, where $\mathbf{J}(\theta)$ is given by (27).

6.3 Optimal Beacon Placement

The accuracy of trilateration estimates of position is influenced by the location of the beacons relative to the point whose coordinates are to be estimated. For example, with eight beacons under the error model we discuss, the NLLS method would perform optimally if the beacons were placed at the corners of a cube, with the point to be estimated in the center. In practice, choices for beacon placement are likely to be limited by topographical considerations. Further research dealing with optimal beacon placement under realistic limitations of specific applications would be valuable.

References

Danial, N.F. and T. Krauthammer, Trilateration adjustment by finite elements, *American Society of Civil Engineers, Journal of the Surveying and Mapping Division,* **106** (1980) 73-93.

Laurila, S.H., *Electronic Surveying in Practice* (John Wiley & Sons, New York, 1983).

Lawson, C.L. and R.I. Hanson, *Solving Least Squares Problems* (Prentice Hall, Englewood Cliffs, New Jersey, 1974).

Leick, A., *GPS Satellite Surveying* (John Wiley & Sons, New York, 1990).

McCullagh, P. and J. Nelder, *Generalized Linear Models*, 2nd ed. (Chapman and Hall, New York, 1989).

McKeown, J.J., Specialized versus general-purpose algorithms for minimizing functions that are sums of squared terms, *Mathematical Programming*, **9** (1975) 57-68.

Mezera, D.F., Trilateration adjustment using unit corrections derived from least squares, *Surveying and Mapping,* **43** (1983) 315-329.

Mikhail, E.M., *Observations and Least Squares* (IEP-Dun-Donnelley, Harper and Row, New York, 1976).

Moffitt, F.H. and H. Bouchard, *Surveying,* 9th ed. (Harper Collins Publishers, New York, 1992).

Numerical Algorithms Group (NAG). Fortran Library (Oxford, U.K., 1991).

Parkinson, B.W. and J.J. Spilker, Jr. (Eds.), *Global Positioning System: Theory and Applications. Vol. I & II.* Progress in Astronautics and Aeronautics. Vol. 163 & 164 (American Institute of Aeronautics and Astronautics (AIAA), Washington, DC, 1996).

Press, W., Teukolsky, S., Vettering, W. and B. Flannery, *Numerical Recipes in FORTRAN,* 2nd ed. (Cambridge University Press, Cambridge, 1992).

Savidge, R.W., Practical Application of Trilateration in Open Pit Coal Mines, *Surveying and Mapping,* **40** (1980) 311-313.

Wolf, P.R., and Ghilani, C.D., *Adjustment Computations: Statistics and Least Squares in Surveying and GIS*, Wiley, New York, 1997

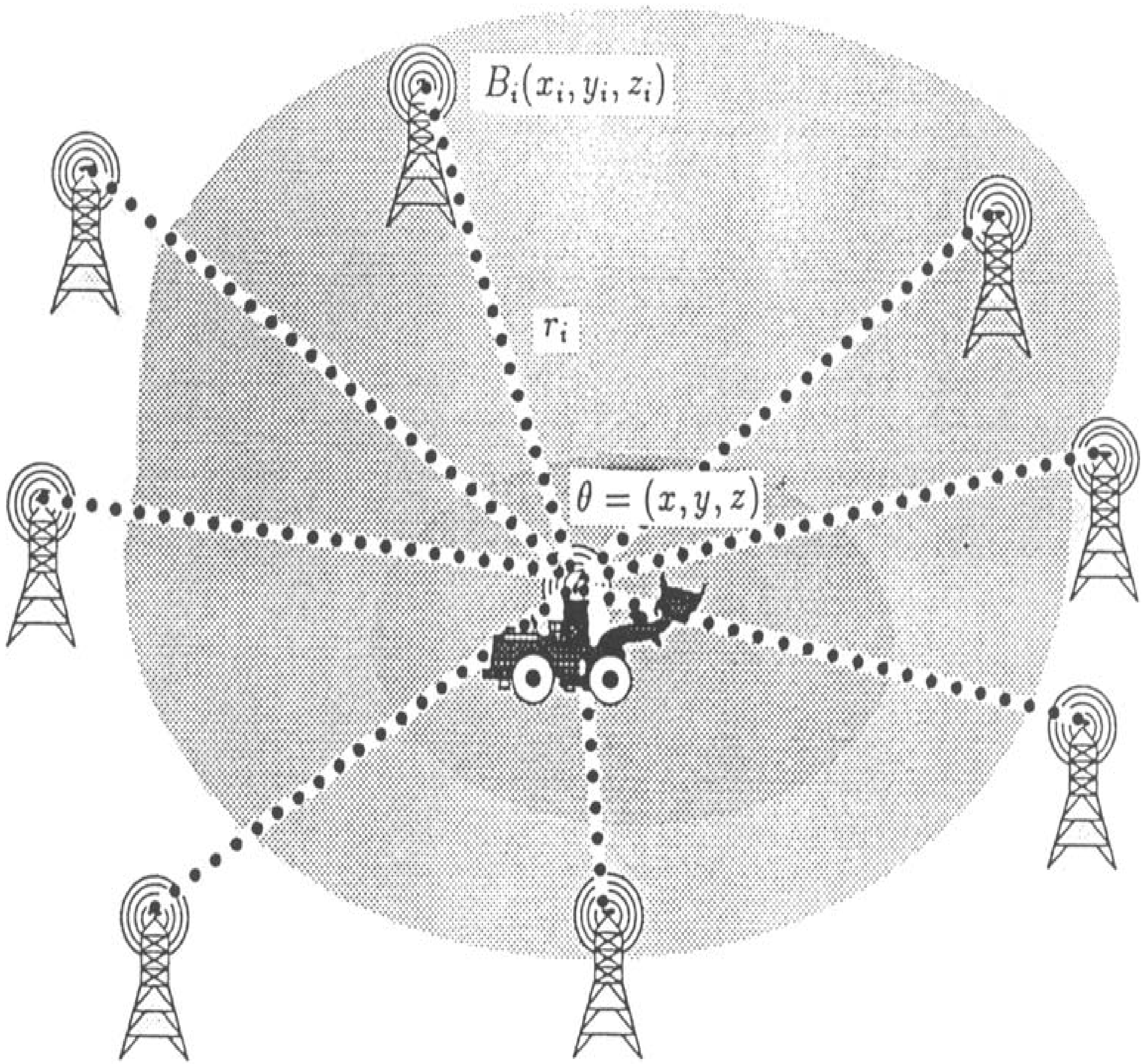

Figure 1: Diagram of the Trilateration Problem.

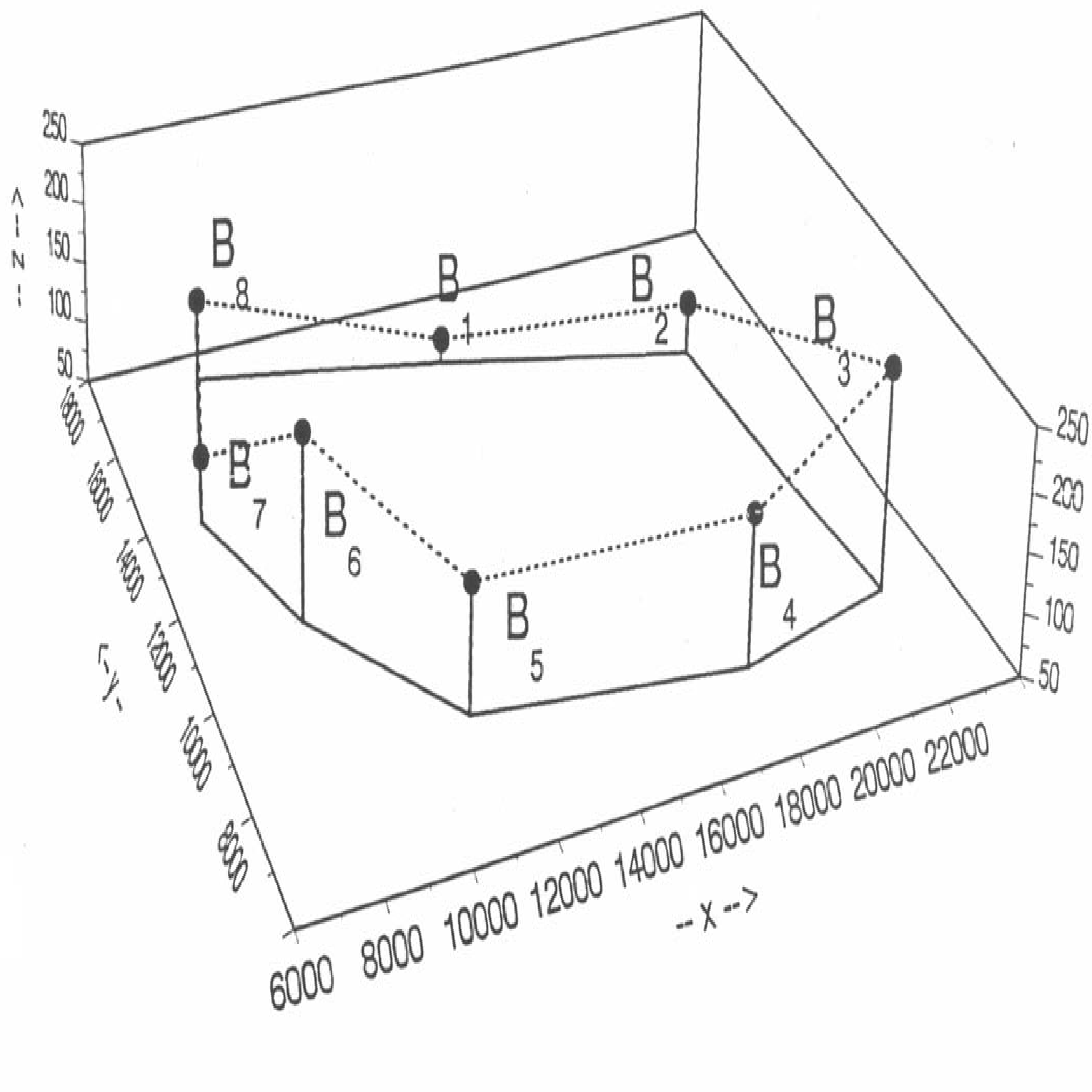

Figure 2: Illustration of Fixed Beacon Locations.

Perspective view of the mine. To obtain the coordinates (in feet), add 460,000 to x, 1,080,000 to y, and 4,600 to z. Note that the vertical $z-$ scale is exaggerated by a factor of approximately 15 relative to the horizontal ones, i.e. the beacons lie very nearly in a plane. The coordinates x, y, and z of the beacons are in the ranges [467400,482230], [1087810, 1097340], and [4670,4831], respectively.

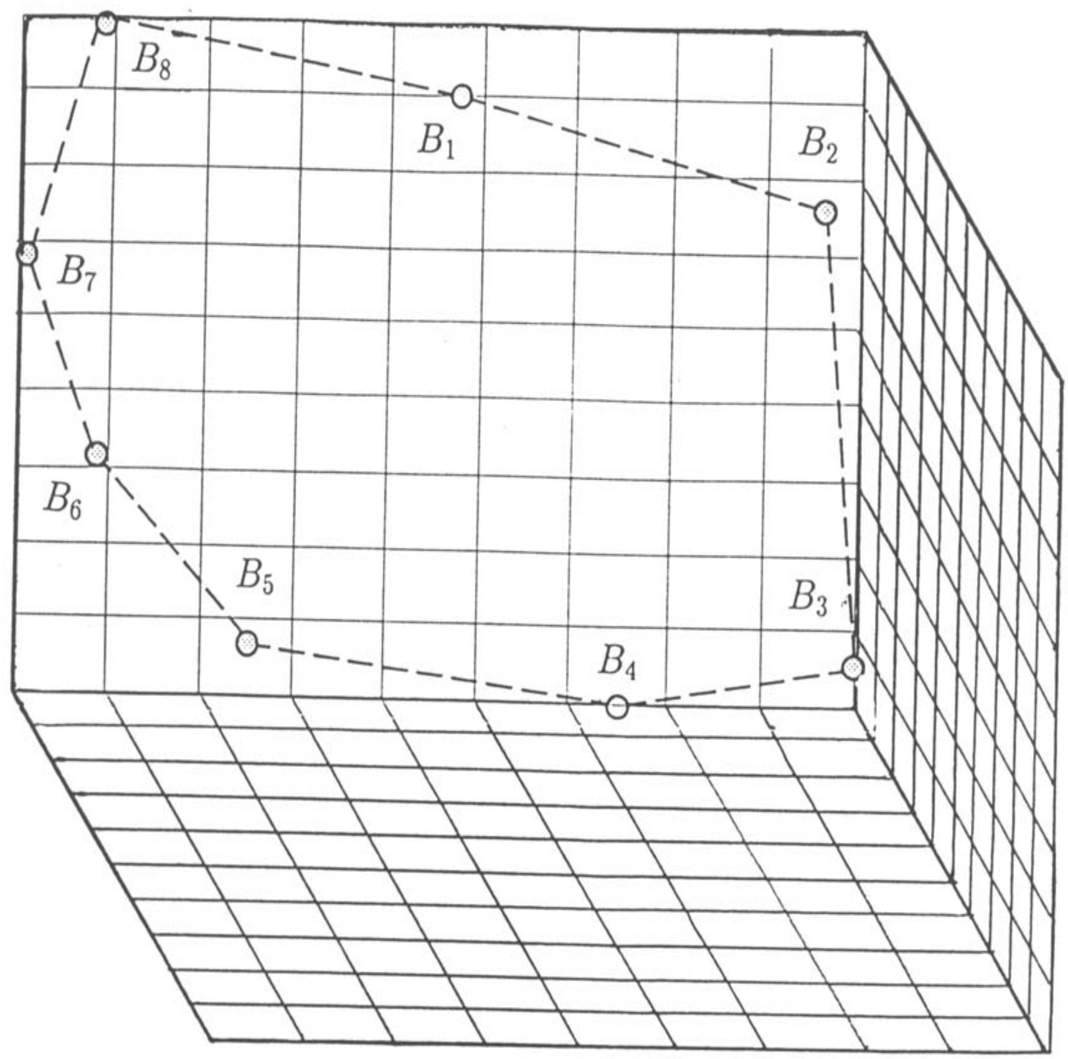

Figure 3: Illustration of Test Grid.

Bird's eye view of the mine. The North, South, East and West boundaries correspond to the extreme positions of the beacons. The top of the grid is 5 feet below the lowest beacon. The coordinates x, y, and z of the target point are in the ranges [467400,482230], [1087810, 1097340], and [4065,4665], respectively.

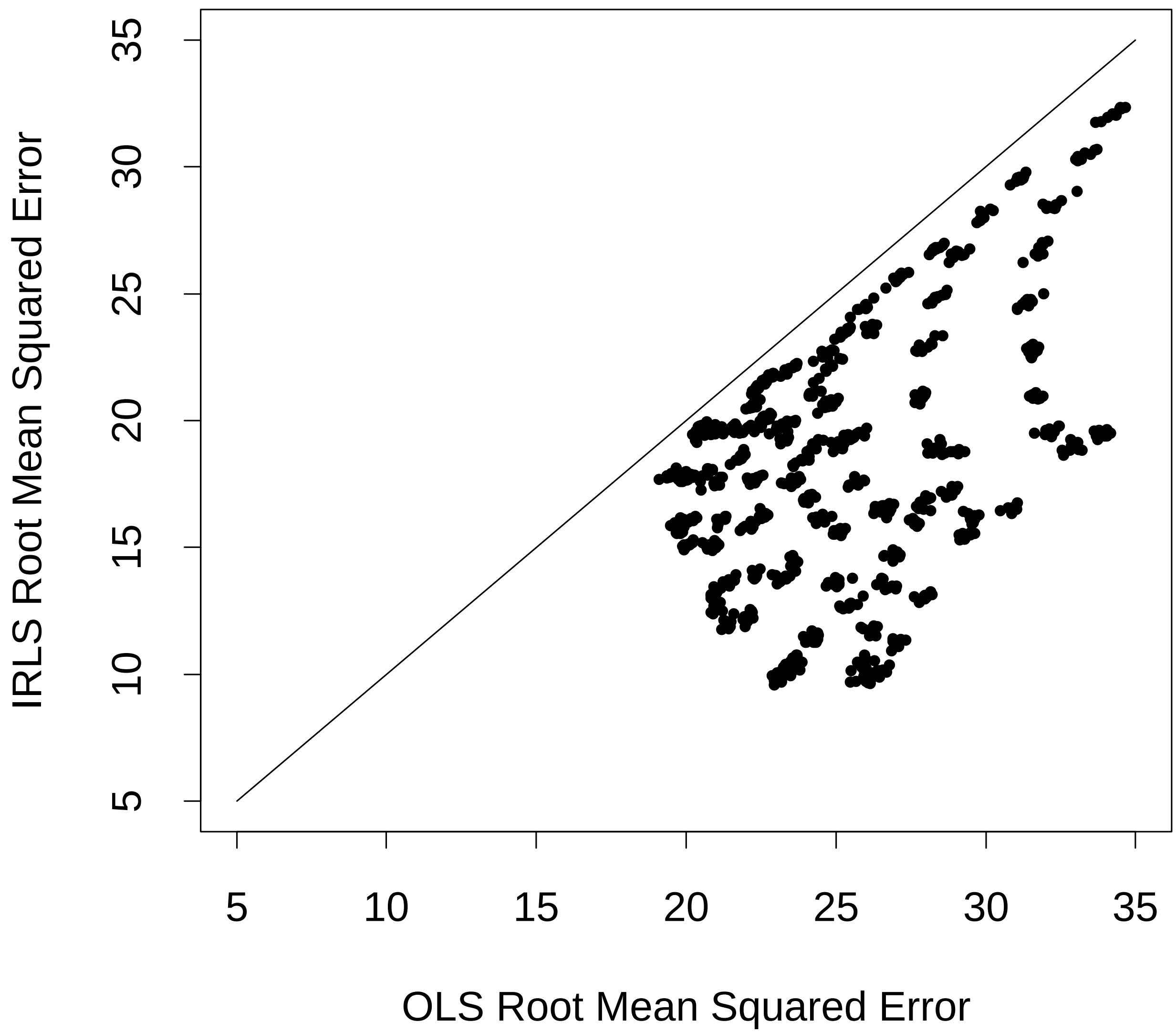
IRLS Root Mean Squared Error
OLS Root Mean Squared Error
5
10
15
20
25
30
35
5
10
15
20
25
30
35

Figure 4:

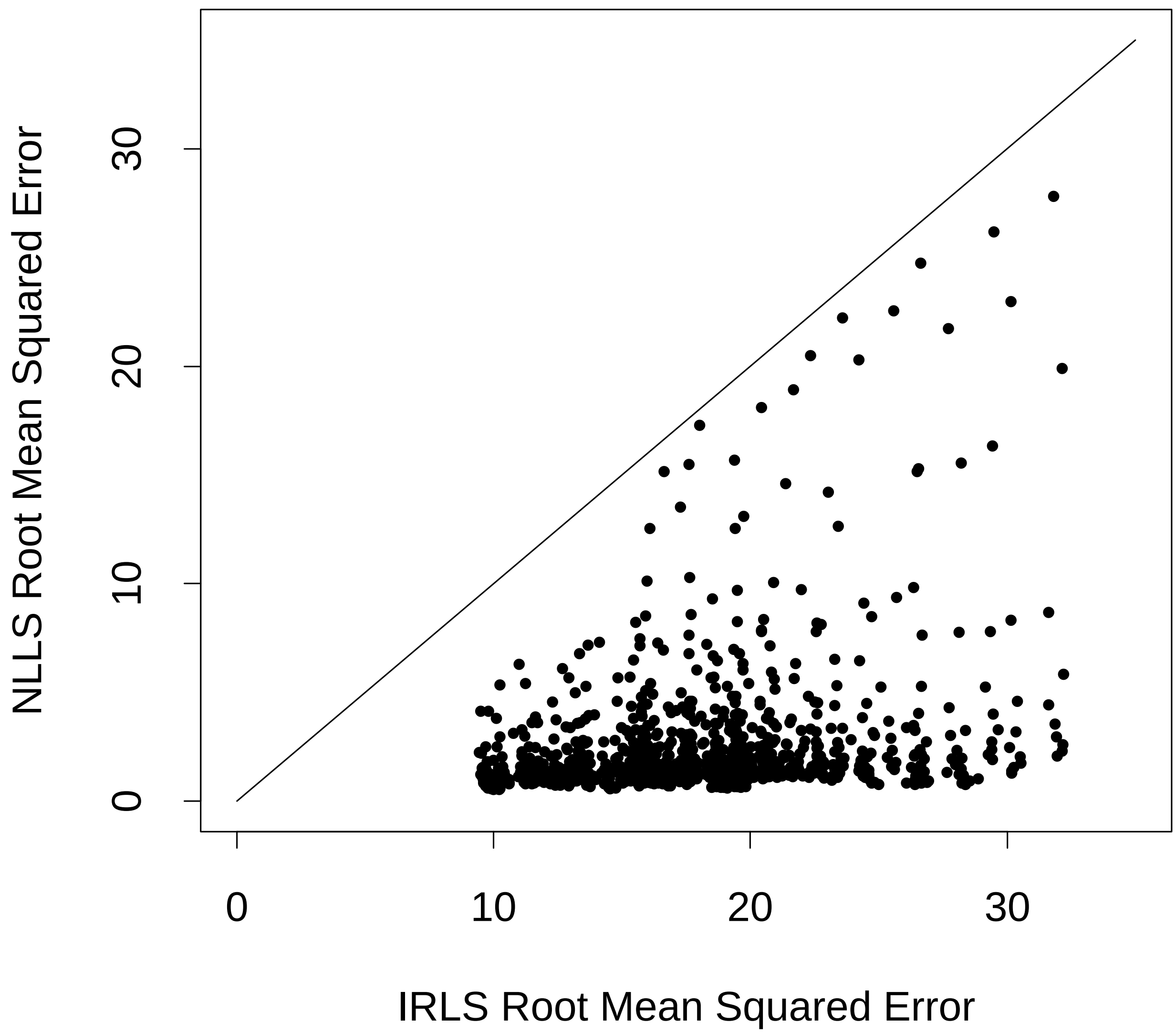

NLLS Root Mean Squared Error
0
10
20
30
0
10
20
30
IRLS Root Mean Squared Error

Figure 5:

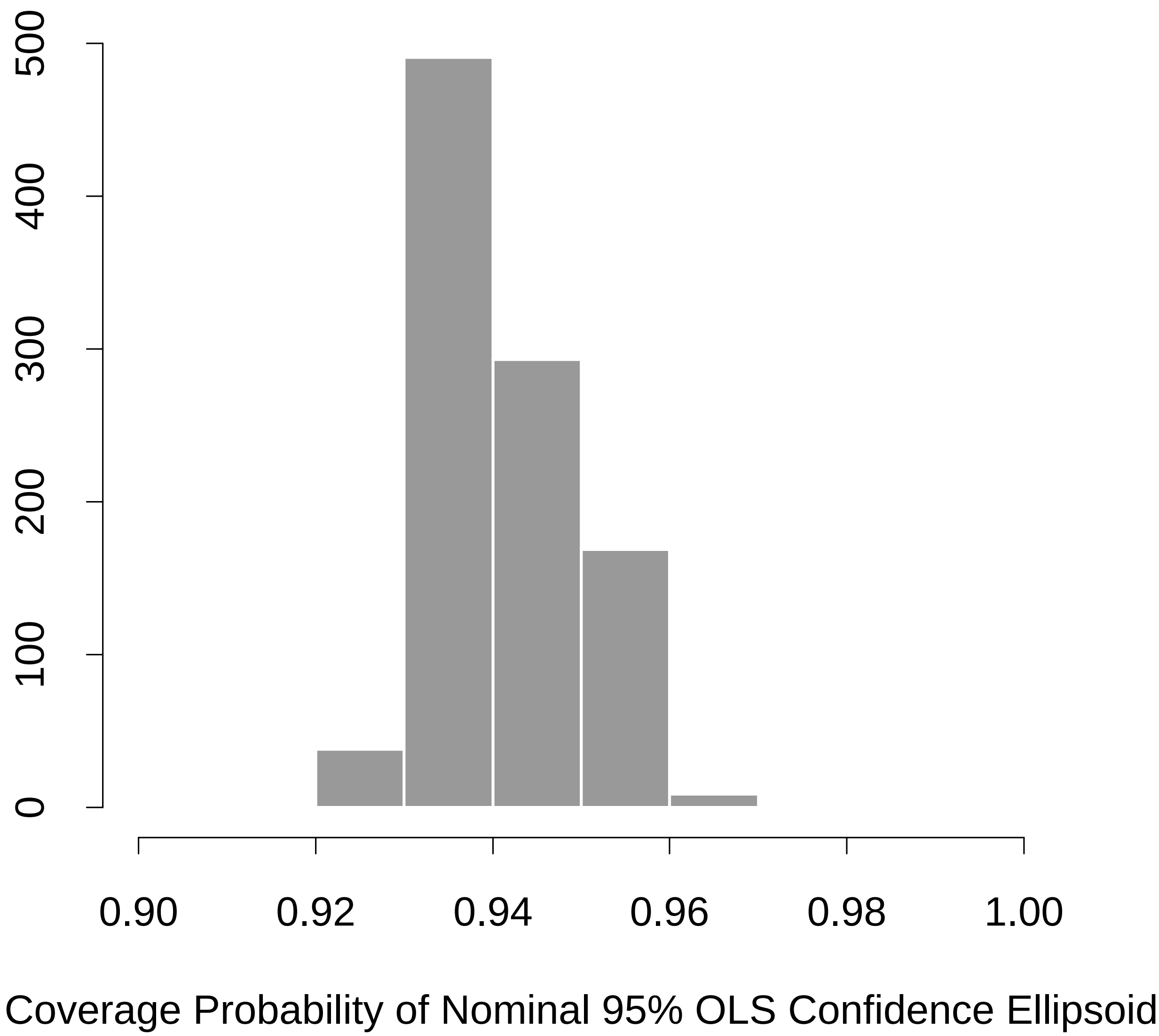
0
100
200
300
400
500
0.90
0.92
0.94
0.96
0.98
1.00
Coverage Probability of Nominal 95% OLS Confidence Ellipsoid

Figure 6:

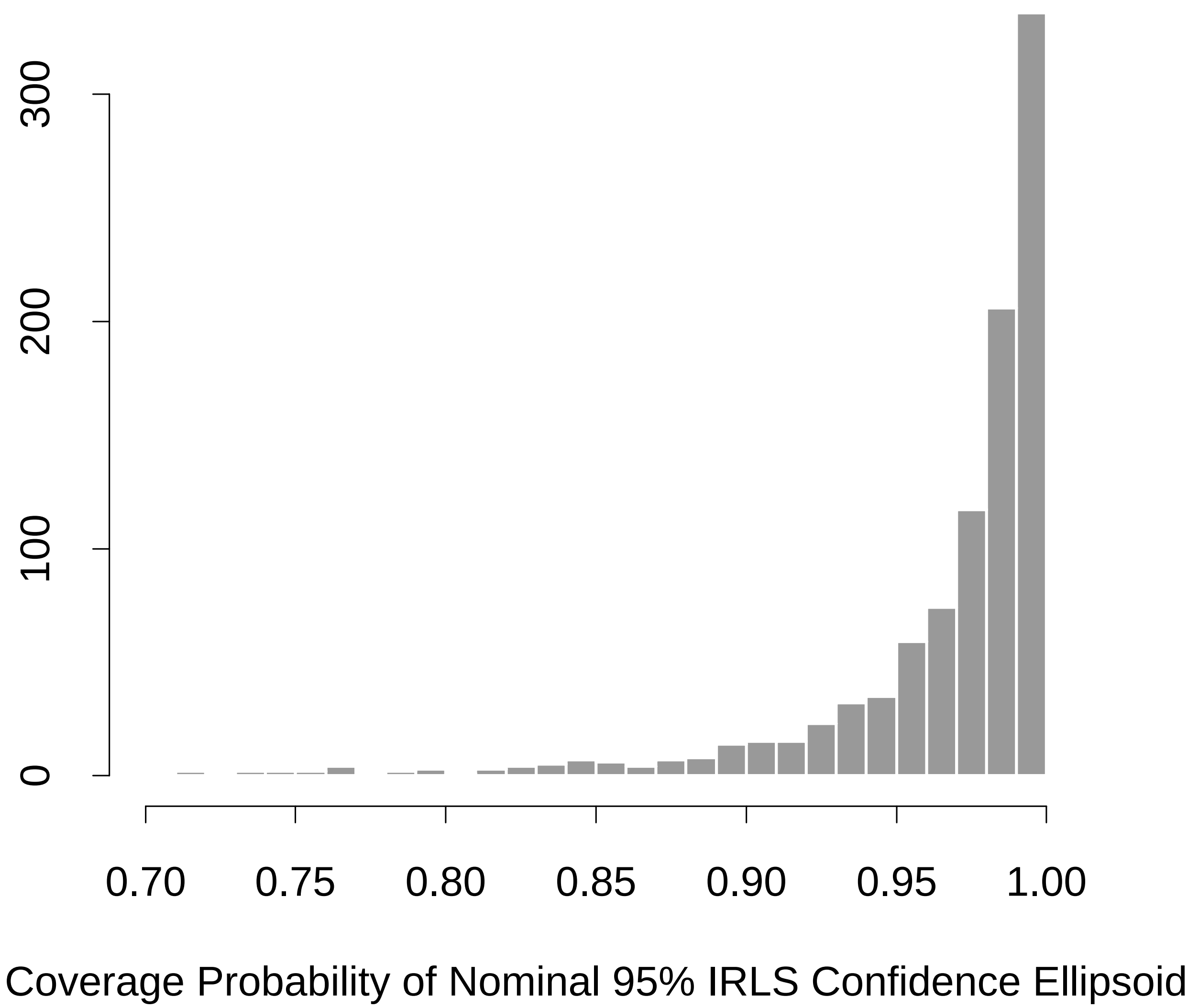
300
200
100
0
0.70
0.75
0.80
0.85
0.90
0.95
1.00
Coverage Probability of Nominal 95% IRLS Confidence Ellipsoid

Figure 7:

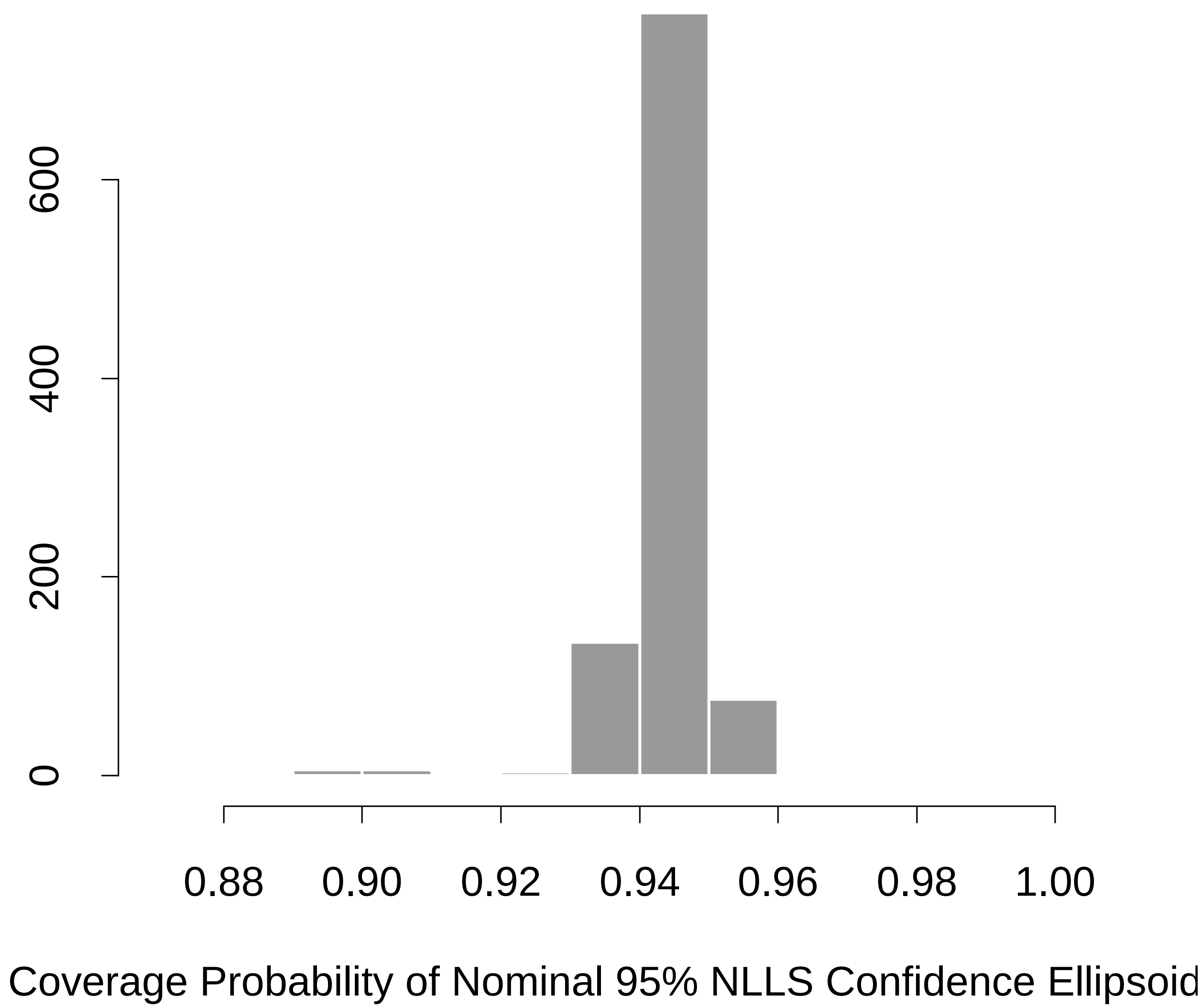

0
200
400
600
0.88
0.90
0.92
0.94
0.96
0.98
1.00
Coverage Probability of Nominal 95% NLLS Confidence Ellipsoid

Figure 8:

Table 1: Coordinates of Fixed Radio Beacon Positions.

Beacon Number	x	y	z
1	475060	1096300	4670
2	481500	1094900	4694
3	482230	1088430	4831
4	478050	1087810	4775
5	471430	1088580	4752
6	468720	1091240	4803
7	467400	1093980	4705
8	468730	1097340	4747

Coordinates are measured from an arbitrary reference point in Western Wyoming. Units are feet.

Table 2: Comparison of methods of estimation.

Estimator	RMSE	Nominal RMSE	Coverage Probability
OLS	25.34	24.12	0.9409
IRLS	18.68	172.92	0.9613
NLLS	3.96	3.78	0.9434

Units are feet.